

# Residual Matrix Product State for Machine Learning

Ye-Ming Meng,<sup>1</sup> Jing Zhang,<sup>2</sup> Peng Zhang,<sup>2</sup> Chao Gao,<sup>1,\*</sup> and Shi-Ju Ran<sup>3,†</sup>

<sup>1</sup>*Department of Physics, Zhejiang Normal University, Jinhua, 321004, China*

<sup>2</sup>*School of Computer Science and Technology, Tianjin University, Tianjin, China*

<sup>3</sup>*Department of Physics, Capital Normal University, Beijing 100048, China*

(Dated: March 29, 2022)

Tensor network (TN), which originates from quantum physics, shows broad prospects in classical and quantum machine learning (ML). However, there still exists a considerable gap of accuracy between TN and the sophisticated neural network (NN) models for classical ML. It is still elusive how far TN ML can be improved by, e.g., borrowing the techniques from NN. In this work, we propose the residual matrix product state (ResMPS) by combining the ideas of matrix product state (MPS) and residual NN. ResMPS can be treated as a network where its layers map the “hidden” features to the outputs (e.g., classifications), and the variational parameters of the layers are the functions of the features of samples (e.g., pixels of images). This is essentially different from NN, where the layers map feed-forwardly the features to the output. ResMPS can naturally incorporate with the non-linear activations and dropout layers, and outperforms the state-of-the-art TN models on the efficiency, stability, and expression power. Besides, ResMPS is interpretable from the perspective of polynomial expansion, where the factorization and exponential machines naturally emerge. Our work contributes to connecting and hybridizing neural and tensor networks, which is crucial to understand the working mechanisms further and improve both models’ performances.

## I. INTRODUCTION

TN, as a mathematic model that is used to describe quantum many-body states [1–4], has been successful applied to machine learning, for instance, the supervised and unsupervised image classification, natural language processing, etc. [5–11]. Although TN is expected to establish the connection between physics and artificial intelligence, and there are several relevant works in the literature [12, 13], despite its high interpretability [14–16], there still exists a considerable gap in performance between TN and NN [17, 18].

For machine learning, TN can realize a non-linear map from features to outputs combined with a local kernel function [5] that maps the features of samples to quantum states in Hilbert space. TN itself only represents a linear map between quantum states. It is an open issue whether the techniques of NN can enhance the performance of TN. Several works in the literature aimed to combine TN and NN, for instance, applying convolutional neural network (CNN) as a feature extractor of TN [7, 17–19], compressing linear layers of deep NN by matrix product operators [20], implementing convolutional operations using TN [21], etc. All these attempts motivate us further to investigate the possible hybridizations of TN and NN.

In this work, we incorporate the information highways (also known as shortcuts) [22, 23], non-linear activations, and dropout into TN (MPS in specific), and propose Residual MPS (ResMPS). The main difference between ResMPS and the existing feed-forward NN is the way of inputting data to the model. For the traditional feed-forward NN, the data is input in the initial step, while for ResMPS, the data are input so that the variational parameters of the layers are the functions of the features of the data.

We give two specific examples of ResMPS dubbed as simple and activated ResMPS, respectively. The results on fashion-MNIST show that the simple ResMPS can achieve the same accuracy as MPS with half of the parameter complexity. For the activated ResMPS, we find that the efficiency and accuracy can be significantly enhanced by introducing the non-linear activations and the dropout layers on the residual terms. Furthermore,

Also, we reveal the model interpretability of sResMPS by polynomial expression technique. The truncated model can obtain considerable accuracy while keeping only a few low-order terms of sResMPS. ResMPS can be interpreted from the perspective of polynomial expansion, where the factorization [24] and exponential machines [25] naturally emerge. Our work shows the possibilities and flexibilities of developing powerful ML models beyond NN or TN from the connections indicated by ResMPS.

## II. RESIDUAL MATRIX PRODUCT STATE

### A. Definition of residual matrix product state

The traditional feed-forward neural network (FNN), including the residual neural network, consists of multiple trainable layers [26]. For supervised learning as an example, the network maps the input sample  $\mathbf{x}$  to the output  $l$ , e.g., the classification of the sample. The typical form of one layer can be written as

$$\mathbf{h}^{[n+1]} = \sigma \left( F^{[n]} \left( \mathbf{h}^{[n]}; \mathbf{W}^{[n]} \right) + \mathbf{b}^{[n]} \right), \quad (1)$$

where  $\mathbf{h}^{[n]}$  denotes the hidden variables that are input to the  $n$ -th layer with  $\mathbf{h}^{[0]} = \mathbf{x}$ ,  $F^{[n]}$  denotes the mapping of the  $n$ -th layer (for example, fully connected, convolution, or pooling layer, etc.). Each layer may consist of variational parameters

\* Corresponding author. Email: [gaochao@zjnu.edu.cn](mailto:gaochao@zjnu.edu.cn)

† Corresponding author. Email: [sjran@cnu.edu.cn](mailto:sjran@cnu.edu.cn)

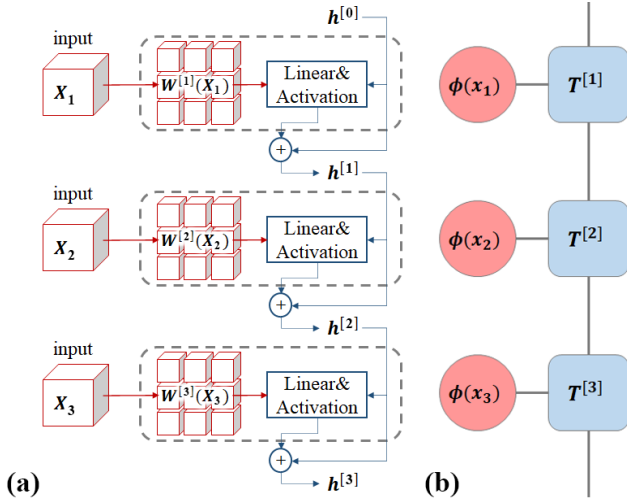


FIG. 1. (a) An illustration of ResMPS containing a three-layer FNN whose variational parameters are the functions of the features  $\mathbf{x}$ . (b) An illustration of a three-tensor MPS, which is contracted with the feature vectors (see Eq. (8)).

$\mathbf{W}^{[n]}$  (weights) and  $\mathbf{b}$  (bias).  $\sigma$  denotes the activation function.

Inspired by matrix product state [27, 28] and residual neural network [22, 23], we propose a novel machine learning architecture dubbed as residual matrix product state (ResMPS). Different from FNN as shown in Eq. (1), ResMPS does not explicitly map the features with a feed-forward network but uses the features to parameterize the variational parameters in the FNN. In this manner, the FNN maps the hidden features to the expected outputs (Fig. 1). Mathematically, the mapping of one layer in a ResMPS can be written as

$$\mathbf{h}^{[n+1]} = \mathbf{h}^{[n]} + f^{[n]}(\mathbf{h}^{[n]}; \mathbf{W}^{[n]}(x_n), \mathbf{b}^{[n]}), \quad (2)$$

where the weights  $\mathbf{W}^{[n]}$  of the  $n$ -th layer are parameterized by the  $n$ -th feature  $x_n$ ,  $\mathbf{h}^{[0]}$  can be simply initialized by ones, and  $f^{[n]}$  denotes the map of the  $n$ -th layer. Similar to FNN [Eq. (1)], this work takes  $f^{[n]}$  in the form as

$$f^{[n]} = \sigma\left(L^{[n]}(\mathbf{h}^{[n]}; \mathbf{W}^{[n]}(x_n)) + \mathbf{b}^{[n]}\right), \quad (3)$$

with  $L^{[n]}$  a linear map and  $\sigma$  the activation. Similar to ResNet, the output of one layer is the addition of the output of  $f^{[n]}$  and the input hidden features in order to form a shortcut of the information flow, for the purpose of avoiding the vanishing/explosion of the gradients. It can be easily seen that one obtains a standard FNN by taking  $\mathbf{h}^{[0]} = \mathbf{x}$  and removing the dependence of  $\mathbf{W}$  on  $\mathbf{x}$ .

## B. ResMPS architectures

In the following, we test two concrete examples of ResMPS, called simple ResMPS (sResMPS) and activated ResMPS (aResMPS). The sResMPS is a multi-linear model

that is equivalent to MPS; it achieves the same accuracy with only half of the parameter complexity compared with the MPS. The aResMPS is a generalized version of sResMPS, whose generalization power is enhanced by introducing non-linear activation functions and dropout in the FNN part. The map of one layer in the sResMPS is written as

$$h_j^{[n+1]} = h_j^{[n]} + \sum_i x_n W_{ij}^{[n]} h_j^{[n]}. \quad (4)$$

The weights of the layers in the FNN possess linear dependence on the features  $\mathbf{x}$ . Bias terms are disabled in this example.

sResMPS is equivalent to a restricted version of MPS, which can achieve identical performance with only half parameter complexity of regular MPS. This will be discussed in detail in Sec. II C.

It can be observed that MPS possesses remarkable representation power. The training error can easily suppress almost 1% [29]. However, the gap between the training and testing accuracies suggests the presence of over-fitting. We propose the activated ResMPS (aResMPS) by incorporating with non-linear activation functions and dropout in order to suppress over-fitting and enhance the generalization power [30]. The map of each layer in the FNN of the aResMPS is more-or-less a fully-connected layer with a shortcut, which reads

$$\mathbf{h}^{[n+1]} = \mathbf{h}^{[n]} + \sigma\left(L^{[n]}(\mathbf{h}^{[n]}) + \mathbf{b}^{[n]}\right), \quad (5)$$

where  $\sigma$  is an activation function. The map  $L^{[n]}$  rely on the feature  $x_n$  in a non-linear way as

$$L^{[n]}(\mathbf{h}^{[n]}) = \sum_{c=1,2} \left[ \xi^{[c]}(x_n) \sum_j W_{ij}^{[n,c]} h_j^{[n]} \right], \quad (6)$$

with  $\xi^{[1]}(x_n) = x_n$  and  $\xi^{[2]}(x_n) = 1 - x_n$ .

The architecture of ResMPS is flexible, including the choice of  $\xi^{[c]}(x_n)$  and the number of channels  $\dim(c)$ . We introduce  $\xi^{[c]}$  to enhance the non-linearity of the aResMPS. We shall emphasize that even for the sResMPS, it represents a non-linear map on the features  $\mathbf{x}$  (but a linear map on the hidden features). For the aResMPS, the map on either the features or the hidden features is non-linear. Indeed, the FNN embedded inside the aResMPS can be replaced by any NN. Here, we choose it as a standard fully-connected network additionally with two channels labeled by  $c$ .

TABLE I. Experimental results on MNIST and Fashion-MNIST dataset. The first 6 models are prune TN architectures, while AlexNet, ResNet, and CNN-PEPS are NN or TN-NN hybrid models. For aResMPS, we use RELU as activation function.

Model	MMIST train	MMIST test	Fashion-MMIST train	Fashion-MMIST test
MPS machine [29]	1.0000	0.9855	0.99	0.88
Unitary tree TN [9]	0.98	0.95	-	-
Tree curtain model [31]	-	-	0.9538	0.8897
Bayesian TN [15]	-	-	0.8950	0.8692
EPS-SBS [17]	-	0.9885	-	0.886
PEPS [18]	-	-	-	0.883
CNN-PEPS [18]	-	-	-	0.912
AlexNet [32]	-	-	-	0.8882
ResNet [32]	-	-	-	0.9339
sResMPS(+dropout)	1.0000	0.9898	0.9920	0.9076
aResMPS(+ReLU,+dropout)	1.0000	0.9900	0.9999	0.9146

Throughout this paper, we choose the ReLU activation function that output the input directly for positive input, and output zero for other cases [33, 34]. Due to of its piecewise linear characteristics, the gradient can directly pass through it without any attenuation or enhancement. Therefore, the ReLU function is suitable for enhancing the non-linearity of the deep networks through improving its expression ability and avoiding the vanishing/explosion of the gradient at the same time. Another trick combined with the residual structure can improve the generalization ability of ResMPS, says dropout, which is used to create an ensemble of networks equivalently, while avoiding the co-adaptation of intermediate variables [35–37]. We impose dropout on the residual terms, e.g.  $\mathbf{h}^{[n+1]} = \mathbf{h}^{[n]} + \text{dropout}(\sigma(\cdot \cdot \cdot))$ . It is worth mentioning that activations and dropout would not take effects to improve the performance if not applied to the residual terms. Therefore, the residual structure makes one of the significant differences between ResMPS and MPS.

### C. Benchmark results

For the MNIST [38] and fashion-MNIST [39] datasets, Table I shows the accuracies of the sResMPS and aResMPS, compared with several established NN [32] and TN models [9, 15, 17, 18, 29, 31]. The representation powers of the MPS and ResMPS models are remarkable, indicated by the high training accuracies. The aResMPS surpasses the probabilistically interpretable Bayesian TN [15] and other TN models, including the two-dimensional TN known as projected-entangled pair state (PEPS) [18], and achieves at (slightly) better accuracy than the CNN-PEPS model, which incorporates CNN as a feature extractor. This precision surpasses the CNN without the stacking architecture, such as AlexNet [32]. The aResMPS still does not beat the ResNet that is formed by stacking multiple convolution layers. We feel promising that the ResMPS models could eventually surpass ResNet by replacing the fully-connected network with more sophisticated ones or staking multiple ResMPSs.

To see the equivalence to the standard MPS, let us introduce

the third-order tensors  $\mathbf{T}^{[n]}$  satisfying

$$T_{1,::}^{[n]} = \mathbf{I}, \quad T_{2,::}^{[n]} = \mathbf{W}^{[n]}. \quad (7)$$

The feature vectors  $\phi(x_n)$  are obtained by the feature map as  $\phi(x_n) = (1, x_n)$ , similar to Refs. [5, 9, 29]. In this way, the sResMPS is then equivalent to the standard MPS formed by these tensors

$$\mathcal{T} = \sum_{\{a\}} \prod_n T_{p_n a_n a_{n+1}}^{[n]} \quad (8)$$

as its tensor-train cores [40] [Fig. 1 (b)]. The numbers of the input and output hidden features for different layers give the two virtual bond dimensions of the MPS, i.e.,  $\{\dim(a_n)\}$ . In this work, we fix  $\dim(a_n) = \chi$  for any  $n$ . The physical dimension of the MPS should match the dimension of the feature vector  $\dim(\phi(x_n)) = \dim(p_n)$ .

For  $\dim(p_n) = 2$ , obviously the number of variational parameters in the sResMPS ( $\sim O(N\chi^2)$  with  $N$  the total number of features) is only half of that in the MPS ( $\sim O(2N\chi^2)$ ). Our numerical simulations show that the accuracies of both models are almost identical. See the training and testing accuracies versus epochs on fashion-MNIST dataset [39] in Fig. 2 (a) with  $\chi = 40$ . This might be because one of the two channels of each tensor in the MPS is much less “activated”. The inset of Fig. 2 (a) shows the average norm of the two channels of different tensors

$$q_p^{[n]} = \frac{1}{\chi^2} \sum_{j=1}^{\chi} \sum_{k=1}^{\chi} |T_{pjk}^{[n]} - \delta_{jk}|, \quad (9)$$

with  $p = 1, 2$  representing the channels. The main contribution to the output is from the second channel. Thus one channel is sufficient to propagate the information to the output.

In physics, the virtual bond dimension  $\chi$  characterizes the representation power of the MPS since it determines the total number of variational parameters and the upper bound of the entanglement entropy that the MPS can carry [1]. Surprisingly, this may not be the case for machine learning. We

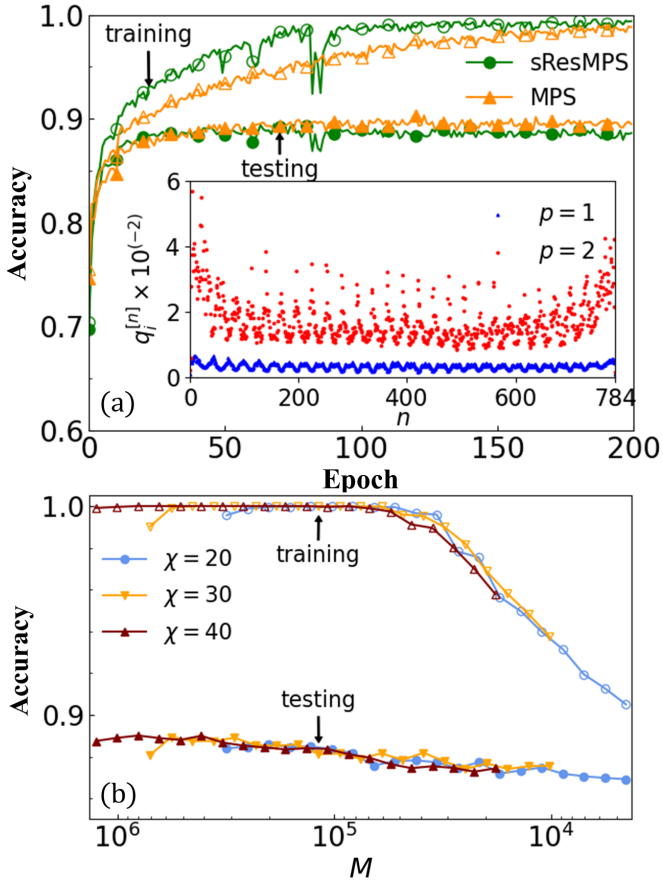


FIG. 2. (a) Training and testing accuracies of sResMPS (without dropout) and MPS versus epochs on the fashion-MNIST dataset. The inset shows the average norm [Eq. (9)] of the two channels in the MPS for different tensors  $n$ . (b) Training and testing accuracies of the sResMPS versus the total number of the unmasked weights in the sResMPS. The left end of each curve corresponds to the unpruned result. Accidentally we found the first few steps of pruning improve the accuracy. Note the total number of sResMPS with  $\chi = 20, 30$ , and  $40$  equals to about  $3 \times 10^5, 7 \times 10^5$  and  $13 \times 10^5$ , respectively.

show this by adding masks on the variational parameters, i.e., pruning [14]. Each parameter is multiplied by a factor that equals zero or one. The parameters multiplied by zeros will be masked. To mask a certain number of parameters, we choose to mask those whose absolute values are relatively small. Then we optimize the unmasked parameters after the masks taking effect.

Fig. 2 (b) shows the accuracies versus the number of unmasked parameters  $M$ . For different virtual bond dimensions ( $\chi = 20, 30$ , and  $40$ ), the results are similar if the number of the unmasked parameters are the same. This suggests that the genuine quantity that characterizes the representation and generalization power is not  $\chi$  but  $M$ . With the given  $\chi$ , it is possible to further reduce the complexity of MPS (and sResMPS) without harming the accuracy. Our results show that the sResMPS reaches the maximal representation power for about  $M \sim O(10^4)$  (training accuracy  $\simeq 99.98\%$ ).

### III. PROPERTIES OF RESIDUAL STRUCTURE

#### A. Avoiding gradient problems by residual terms

A typical MPS architecture that is designed for pattern recognition contains hundreds of tensor cores, and thus will probably encounter the gradient vanishing/exploding problems. For this reason, some existing MPS schemes apply a DMRG-like algorithm where the MPS is kept in the canonical form [5, 6, 10, 41]. In these attempts, however, the accuracy is sensitive to the hidden features' dimensions (virtual bonds). Recently, an MPS algorithm based on automatic gradient technique [29] can reach relatively higher accuracies than the previous ones, while its performance is not sensitive to the virtual dimensions. This leaves a puzzle why such a deep network can well avoid the gradient problems.

To answer this question, we construct the tensor cores to satisfy a special form given by Eq. (7). The identity in  $T_{1,\dots}^{[n]}$  plays the role of “highway” to pass the information from the previous tensor core directly to the latter ones. The components  $T_{2,\dots}^{[n]}$  represent the residual terms, which should be  $\ll O(1)$ . The application of residual condition yields that each layer of ResMPS can easily express identity mapping. In other words, the architecture of ResMPS satisfies the identity parameterization [22, 23, 42].

To further demonstrate the role of identity parameterization in ResMPS, we use Gaussian distributions with zero mean and standard deviation  $\varepsilon$  to randomly initialize the elements of  $T_{2,\dots}^{[n]}$ . Fig. 3 shows the testing accuracy at the 10-th, 20-th and 50-th epoch. For a sufficiently small  $\varepsilon$ , the accuracy can converge fast and stably. However, when  $\varepsilon$  becomes relatively large, say  $O(10^{-1})$  as illustrated by the red region, the gradients become unstable. Consequently, the accuracy stays around 0.1 and cannot be improved by the training process. Note that it would be unstable in most cases (like those with relatively large  $\varepsilon$ ) if one does not use the identity parameterization but entirely randomly initializes the whole  $T$ .

#### B. Relations to polynomial expansion

The forward propagation of the sResMPS (4) is fully linear on the hidden features. Applying the maps to the initial hidden features  $\mathbf{h}_0$  in sequence, we can rewrite the output hidden features in an expansive form [Fig. 4 (b)] as

$$\begin{aligned} \mathbf{h}^{[N]} &= \left( \mathbf{I} + x_N \mathbf{W}^{[N]} \right) \dots \left( \mathbf{I} + x_2 \mathbf{W}^{[2]} \right) \left( \mathbf{I} + x_1 \mathbf{W}^{[1]} \right) \mathbf{h}^{[0]} \\ &= \sum_{k=0}^N \mathbf{M}^{[k]} \mathbf{h}^{[0]}, \end{aligned} \quad (10)$$

with  $N$  the total number of the features  $\mathbf{x}$ . The output  $\mathbf{h}^{[N]}$  is the stack of  $N$  terms. The zeroth term satisfies  $\mathbf{M}^{[0]} = \mathbf{I}$ , which is the result of the information highway from the first input hidden features to the output. The term  $\mathbf{M}_1 = \sum_{\alpha=1}^N x_{\alpha} \mathbf{W}^{[\alpha]}$  is the part in ResMPS linear on the

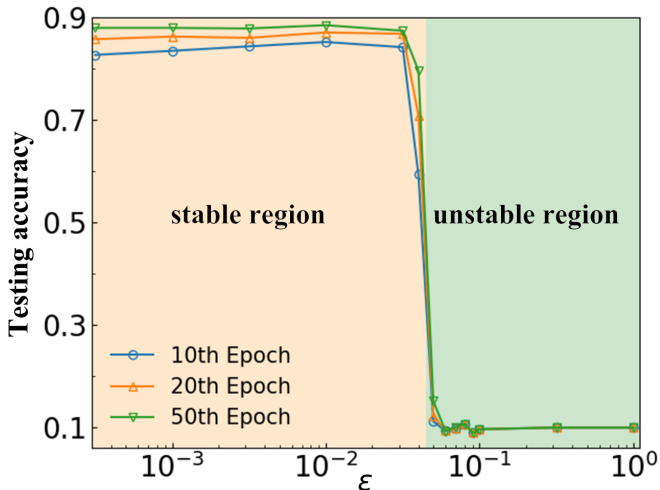


FIG. 3. The testing accuracies of the sResMPS versus  $\varepsilon$  (the standard deviation of the initial residual part) on fashion-MNIST dataset. We fix the number of epochs to be 10, 20, and 50 as examples. The network can be trained stably when  $\varepsilon$  is small. Otherwise, the training process will encounter gradient vanishing (or explosion) problems. The stable and unstable regions are illustrated by green and red, respectively. Note that for the red region, The value of the network elements diverges, but due to some numerical reasons, the simulation still gives some predictions, so the accuracy tends to 0.1.

features  $\mathbf{x}$ . Generally speaking, the  $k$ -th term contains the  $k$ -th order contributions from  $\mathbf{x}$ , i.e.,

$$\mathbf{M}_k = \sum_{\alpha_1 \dots \alpha_k=1}^N G_{\alpha_1 \dots \alpha_k} x_{\alpha_1} \dots x_{\alpha_k} \mathbf{W}^{[\alpha_1]} \dots \mathbf{W}^{[\alpha_k]} \quad (11)$$

$$G_{a_1, a_2, \dots, a_n} = \begin{cases} 1, & a_1 > a_2 > \dots > a_n \\ 0, & \text{otherwise.} \end{cases} \quad (12)$$

This formula is a specific form of the Exponential Machines [25]. Due to their essential similarity, the algebraic properties of Exponential Machines are also valid for sResMPS. For instance, the output feature  $\mathbf{h}^{[N]}$  is a linear mapping concerning the initial hidden feature  $h_0$ , and a multilinear mapping concerning the feature  $\mathbf{x}$ .

From the residual condition (see Eq. (7) with  $|\mathbf{W}^{[n]}| \ll O(10^{-1})$ ), the contributions from the higher-order terms of (11) should decay exponentially with  $k$ . Therefore, we can naturally define a set of lower-order effective models by retaining the first few terms. For example, by only keeping the zeroth- and first-order terms in Eq. (11), we simply get a model whose output features are linear to both the hidden features and features of the samples. Keeping the zeroth, linear, and quadratic terms, the resulting model can be written as

$$\mathbf{h}^{[N](2)} = \left( \mathbf{I} + \sum_{\alpha=1}^N x_{\alpha} \mathbf{W}^{[\alpha]} + \sum_{\alpha, \beta=1}^N G_{\alpha, \beta} x_{\alpha} x_{\beta} \mathbf{W}^{[\alpha]} \mathbf{W}^{[\beta]} \right) \mathbf{h}^{[0]}. \quad (13)$$

This model is similar to Factorization Machines [24] and the polynomial NN [43].

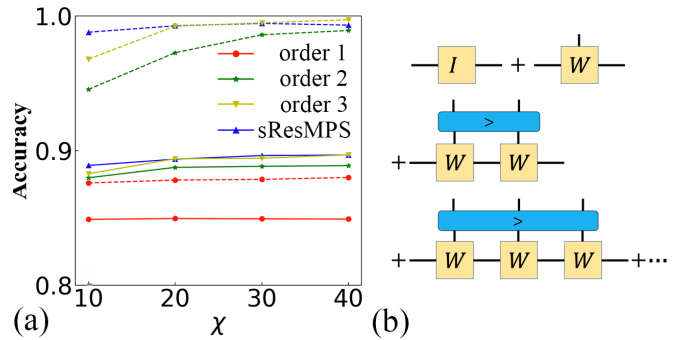


FIG. 4. (a) Training and testing accuracies versus  $\chi$  by taking different orders in the expansion form. (b) The illustration of the polynomial expansion picture of the sResMPS. See Eq. (11).

Fig. 4 (a) shows the differences between the accuracies of several lower-order models and the sResMPS. This implies that the significant contribution in the sResMPS comes from a few lower-order terms, especially the linear term. As the order increases, the cost of directly computing Eq. (10) increases exponentially. Therefore, truncating the order of expansion is not economical. ResMPS adopts a different and efficient scheme for retaining all higher-order interactions.

#### IV. CONCLUSION

In summary, we propose ResMPS by incorporating MPS with the information highways, non-linear activations, and dropout. On the one hand, different from FNN, the variational parameters in ResMPS are replaced by adjustable functions. For FNN, features are inputted at the first layer of the network. For ResMPS, however, features are divided and inputted into the weight matrices of each layer, which is inherited from MPS. On the other hand, thanks to the introduction of neural network structures, ResMPS has a more vital expression ability than MPS. We put forward two specific practices of ResMPS.

The first derived architecture is coined sResMPS, the simple linear version of ResMPS. By comparing MPS' learning performance on the fashion-MNIST dataset, we reveal the channel redundancy of MPS. sResMPS discards the redundant channel. Consequently, it can achieve consistent accuracy when the parameters are halved.

The second one is coined aResMPS, the general ResMPS equipped with activation and dropout layers. We also compare the model with several TN and NN models on fashion-MNIST dataset. The activation and dropout layer enhanced the non-linearity and generalization ability of the model, respectively. As a result, aResMPS surpass the state-of-the-art TN methods and AlexNet in terms of accuracy, although still inferior to ResNet that is formed by stacking multiple convolution layers. Going beyond present aResMPS to achieve higher accuracy, e.g. replacing the weight matrices with convolution layers, is a valuable improvement direction of ResMPS.

The perspectives of the residual network derived the poly-

nomial expansion of ResMPS. The benefits are two-fold. Firstly, We give the condition of vanishing/explosion of the gradients of ResMPS, which helps guide the feature design of MPS and ResMPS algorithms with stable convergence. Secondly, it establishes the equivalence between MPS and polynomial networks such as Factorization Machines and Exponential Machines. Further numerical evidence suggests that high-order terms' contribution is insignificant, which helps build a deeper understanding of MPS and ResMPS.

Are other NN structures (e.g., convolution and pooling layers) compatible with ResMPS? Is it possible to propose a ResMPS structure based on general NN structures (e.g., Tree TN or Projected Entangled-Pair States)? These problems are

worthy of further study.

## V. ACKNOWLEDGEMENTS

Y.-M. M and C.G. are supported by NSFC (Grant No. 1183501 and No. 12074342), and Zhejiang NSFC (Grant No. LY21A040004). S.-J.R is supported by NSFC (Grant No. 12004266 and No. 11834014), Beijing Natural Science Foundation (No. 1192005 and No. Z180013), Foundation of Beijing Education Committees (No. KM202010028013), and the Academy for Multidisciplinary Studies, Capital Normal University. J.Z. and P.Z. are supported by NSFC (Grant No. 61772363).

- 
- [1] U. Schollwöck, The density-matrix renormalization group in the age of matrix product states, *Annals of Physics* **326**, 96 (2011).
- [2] S.-J. Ran, E. Tiritto, C. Peng, X. Chen, L. Tagliacozzo, G. Su, and M. Lewenstein, *Tensor Network Contractions* (Springer International Publishing, 2020).
- [3] F. Verstraete, V. Murg, and J. Cirac, Matrix product states, projected entangled pair states, and variational renormalization group methods for quantum spin systems, *Advances in Physics* **57**, 143 (2008).
- [4] G. Evenbly and G. Vidal, Tensor network states and geometry, *Journal of Statistical Physics* **145**, 891 (2011).
- [5] E. Stoudenmire and D. J. Schwab, Supervised learning with tensor networks, in *Advances in Neural Information Processing Systems 29*, edited by D. D. Lee, M. Sugiyama, U. V. Luxburg, I. Guyon, and R. Garnett (Curran Associates, Inc., 2016) pp. 4799–4807.
- [6] Z.-Y. Han, J. Wang, H. Fan, L. Wang, and P. Zhang, Unsupervised generative modeling using matrix product states, *Physical Review X* **8**, 10.1103/physrevx.8.031012 (2018).
- [7] I. Glasser, N. Pancotti, and J. I. Cirac, From probabilistic graphical models to generalized tensor networks for supervised learning, 1806.05964v2.
- [8] S. Cheng, L. Wang, T. Xiang, and P. Zhang, Tree tensor networks for generative modeling, *Physical Review B* **99**, 10.1103/physrevb.99.155131 (2019).
- [9] D. Liu, S.-J. Ran, P. Wittek, C. Peng, R. B. García, G. Su, and M. Lewenstein, Machine learning by unitary tensor network of hierarchical tree structure, *New Journal of Physics* **21**, 073059 (2019).
- [10] Z.-Z. Sun, S.-J. Ran, and G. Su, Tangent-space gradient optimization of tensor network for machine learning, *Physical Review E* **102**, 10.1103/physreve.102.012152 (2020).
- [11] P. Zhang, Z. Su, L. Zhang, B. Wang, and D. Song, A quantum many-body wave function inspired language modeling approach, in *Proceedings of the 27th ACM International Conference on Information and Communications Security* (ACM, 2018).
- [12] J. Chen, S. Cheng, H. Xie, L. Wang, and T. Xiang, Equivalence of restricted boltzmann machines and tensor network states, *Physical Review B* **97**, 10.1103/physrevb.97.085104 (2018).
- [13] V. Khulkov, A. Novikov, and I. Oseledets, Expressive power of recurrent neural networks, in *International Conference on Learning Representations* (2018).
- [14] Y. Levine, O. Sharir, N. Cohen, and A. Shashua, Quantum entanglement in deep learning architectures, *Phys. Rev. Lett.* **122**, 065301 (2019).
- [15] S.-J. Ran, Bayesian tensor network with polynomial complexity for probabilistic machine learning, 1912.12923v2.
- [16] J. Martyn, G. Vidal, C. Roberts, and S. Leichenauer, Entanglement and tensor networks for supervised image classification, 2007.06082v1.
- [17] I. Glasser, N. Pancotti, and J. I. Cirac, From probabilistic graphical models to generalized tensor networks for supervised learning, *IEEE Access* **8**, 68169 (2020).
- [18] S. Cheng, L. Wang, and P. Zhang, Supervised learning with projected entangled pair states, 2009.09932v1.
- [19] D. Liu, Z. Yao, and Q. Zhang, Quantum-classical machine learning by hybrid tensor networks, 2005.09428v1.
- [20] Z.-F. Gao, S. Cheng, R.-Q. He, Z. Y. Xie, H.-H. Zhao, Z.-Y. Lu, and T. Xiang, Compressing deep neural networks by matrix product operators, *Phys. Rev. Research* **2**, 023300 (2020).
- [21] P. Blagojevich and A. H. Phan, Deep convolutional tensor network, 2005.14506v1.
- [22] K. He, X. Zhang, S. Ren, and J. Sun, Identity mappings in deep residual networks, in *Computer Vision – ECCV 2016* (Springer International Publishing, 2016) pp. 630–645.
- [23] K. He, X. Zhang, S. Ren, and J. Sun, Deep residual learning for image recognition, 2016 IEEE Conference on Computer Vision and Pattern Recognition (CVPR) , 770 (2016).
- [24] S. Rendle, Factorization machines, in *2010 IEEE International Conference on Data Mining* (IEEE, 2010).
- [25] A. Novikov, M. Trofimov, and I. V. Oseledets, Exponential machines, in *ICLR* (2017).
- [26] H. B. Demuth, M. H. Beale, O. De Jess, and M. T. Hagan, *Neural Network Design*, 2nd ed. (Martin Hagan, Stillwater, OK, USA, 2014).
- [27] I. V. Oseledets, Tensor-train decomposition, *SIAM Journal on Scientific Computing* **33**, 2295 (2011), <https://doi.org/10.1137/090752286>.
- [28] D. Perez-García, F. Verstraete, M. M. Wolf, and J. I. Cirac, Matrix product state representations, *Quantum Information and Computation* **7**, 401 (2007).
- [29] S. Efthymiou, J. Hidary, and S. Leichenauer, Tensor network for machine learning, arXiv preprint arXiv:1906.06329 (2019).
- [30] J. Gao, L.-F. Qiao, Z.-Q. Jiao, Y.-C. Ma, C.-Q. Hu, R.-J. Ren, A.-L. Yang, H. Tang, M.-H. Yung, and X.-M. Jin, Experimental

- machine learning of quantum states, *Physical Review Letters* **120**, [10.1103/physrevlett.120.240501](https://doi.org/10.1103/physrevlett.120.240501) (2018).
- [31] E. M. Stoudenmire, Learning relevant features of data with multi-scale tensor networks, *Quantum Science and Technology* **3**, 034003 (2018).
- [32] K. Meshkini, J. Platos, and H. Ghassemian, An analysis of convolutional neural network for fashion images classification (fashion-mnist), in *Proceedings of the Fourth International Scientific Conference “Intelligent Information Technologies and Industry (IITI’19)”* edited by S. Kovalev, V. Tarassov, V. Snasel, and A. Sukhanov (Springer International Publishing, Cham, 2020) pp. 85–95.
- [33] X. Glorot, A. Bordes, and Y. Bengio, Deep sparse rectifier neural networks, in *14th International Conference on Artificial Intelligence and Statistics*, Vol. 15 (2011) pp. 315–323.
- [34] A. F. Agarap, Deep learning using rectified linear units (relu), [1803.08375](https://doi.org/10.1803.08375).
- [35] N. Srivastava, G. Hinton, A. Krizhevsky, I. Sutskever, and R. Salakhutdinov, Dropout: A simple way to prevent neural networks from overfitting, *J. Mach. Learn. Res.* **15**, 1929–1958 (2014).
- [36] P. Baldi and P. J. Sadowski, Understanding dropout, in *Advances in Neural Information Processing Systems*, Vol. 26, edited by C. J. C. Burges, L. Bottou, M. Welling, Z. Ghahramani, and K. Q. Weinberger (Curran Associates, Inc., 2013) pp. 2814–2822.
- [37] W. Zaremba, I. Sutskever, and O. Vinyals, Recurrent neural network regularization, [1409.2329](https://arxiv.org/abs/1409.2329).
- [38] Y. LECUN, The mnist database of handwritten digits, <http://yann.lecun.com/exdb/mnist/>.
- [39] H. Xiao, K. Rasul, and R. Vollgraf, Fashion-mnist: a novel image dataset for computer vision, in *International Conference on Computer-Aided Design (ICCAD)* (2017), [cs.LG/1708.07747](https://arxiv.org/abs/cs.LG/1708.07747).
- [40] T. G. Kolda and B. W. Bader, Tensor decompositions and applications, *SIAM Review* **51**, 455 (2009).
- [41] S. R. White, Density matrix formulation for quantum renormalization groups, *Phys. Rev. Lett.* **69**, 2863 (1992).
- [42] M. Hardt and T. Ma, Identity Matters in Deep Learning, *ICLR* (2016), [1611.04231](https://arxiv.org/abs/1611.04231) [cs.LG].
- [43] L.-L. Huang, A. Shimizu, Y. Hagihara, and H. Kobatake, Face detection from cluttered images using a polynomial neural network, *Neurocomputing* **51**, 197 (2003).